

Protonation state and fine structure of active site determine the reactivity of dehydratase: hydration and isomerization of β -myrcene catalyzed by linalool dehydratase/isomerase from *Castellaniella defragrans*

Baoping Ling^{a,b}, Xiya Wang^b, Hao Su^b, Rutao Liu^{b,*}, Yongjun Liu^{b,*}

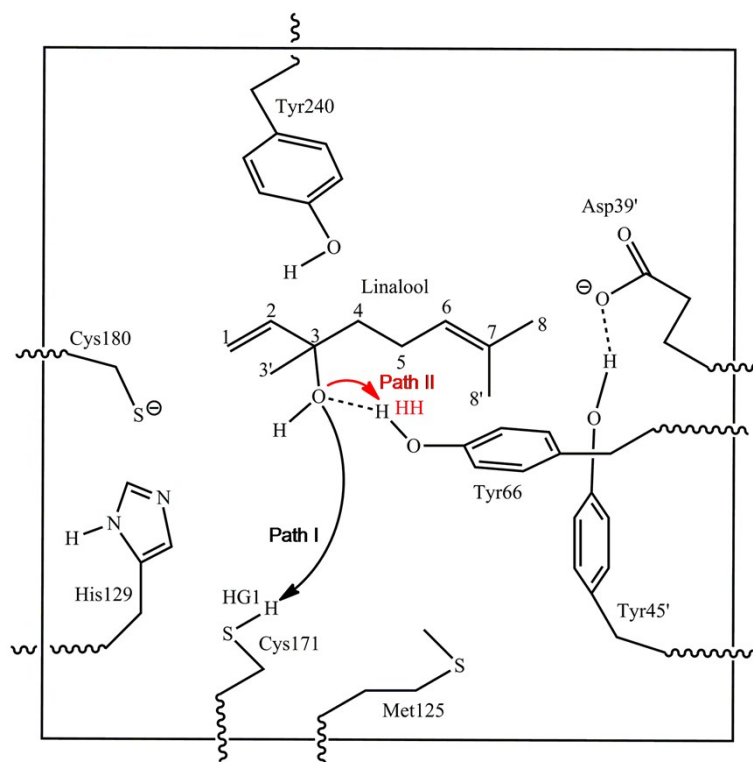
^a *School of Chemistry and Chemical Engineering, Qufu Normal University, Qufu, Shandong 273165, China*

^b *School of Chemistry and Chemical Engineering & School of Environmental Science and Engineering, Shandong University, Jinan, Shandong 250100, China*

(Corresponding author: E-mail: yongjunliu_1@sdu.edu.cn; Fax: +86 53188564464)

Table S1 The relative entropy effects and empirical dispersion corrections for Model II. The reported energies are relative to the corresponding energy of R.

Species	T×ΔS (kcal/mol)	B3LYP-D3 (kcal/mol)
R	0.00	0.00
TS1	-0.62	-1.25
IM1	-0.19	-1.30
TS2	-1.79	-3.29
IM2	-0.96	-0.68
TS3	-2.27	-2.04
IM3	-0.31	-0.18
TS4	0.00	-1.41
P	-1.61	-1.52
TS2b	2.02	-3.46
Pb	-1.93	-1.63
TS4c	-1.13	-0.69
IM4c	-0.56	-0.54
TS5c	-0.22	-0.14
R'	0.19	0.18



Scheme S1 Selected QM region for the QM/MM calculations (model I). The calculated reaction pathways, path I and path II, according to the proposal of Nestl *et al.*¹³, are represented by black and red arrows, respectively.

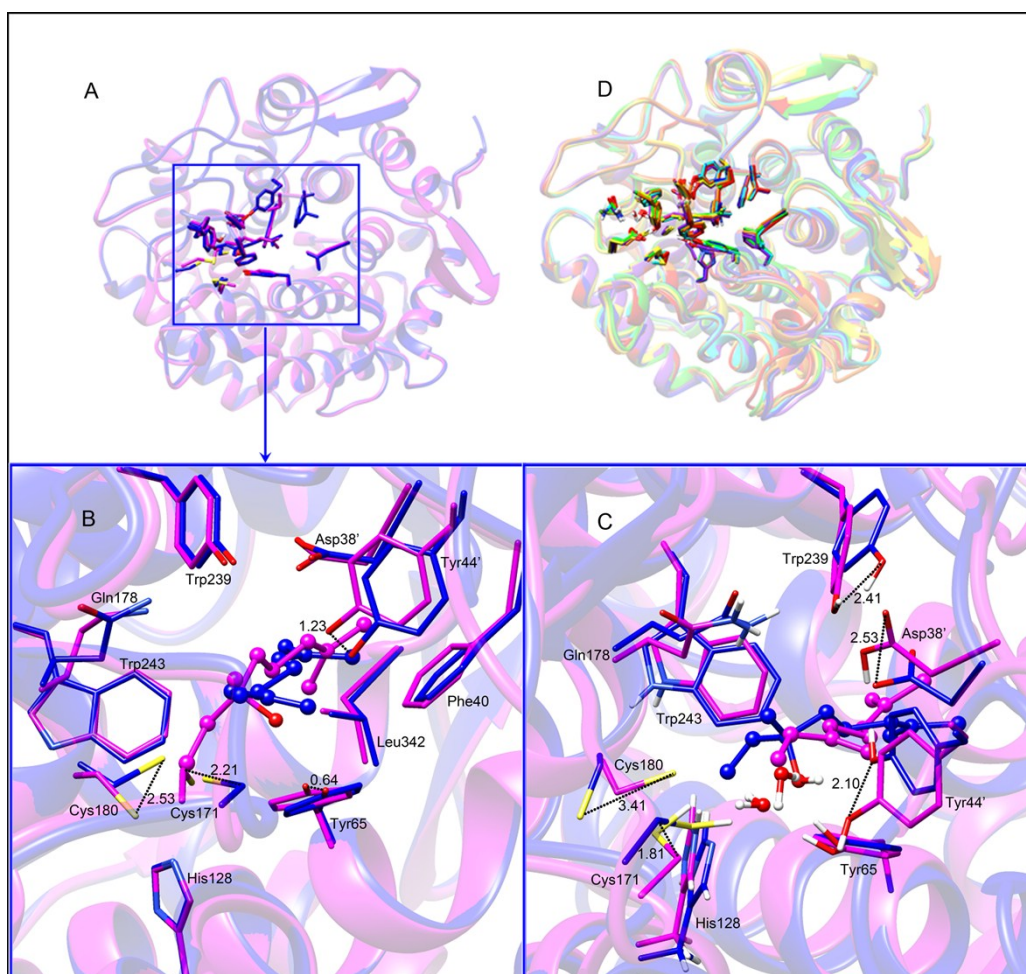


Figure S1 (A) Superimposition of subunits of the crystal structures from 5HSS and 5G1U; Close views of the superimpositions of the active sites from two crystal structures (B) and two QM/MM optimized structures (C), 5HSS and 5G1U are shown in blue and magenta, respectively. (D) Overlap of seven snapshots extracted from MD trajectories of model II at 4 (red), 5 (orange), 6 (yellow), 7 (green), 8 (cyan), 9 (blue) and 10 (purple) ns.

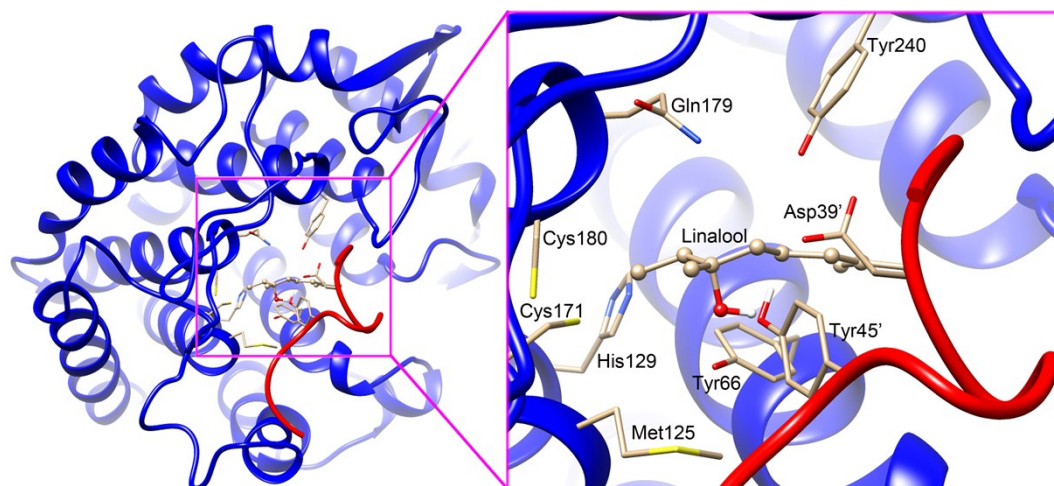


Figure S2 Crystal structure and active site of linalool dehydratase/isomerase from *Castellaniella defragrans* with (*S*)-linalool (PDB code: 5G1U). Chain A and the segment of chain C are shown in the blue and red ribbons, respectively. Substrate linalool is obtained by manually modifying geraniol. All distances are given in angstroms.

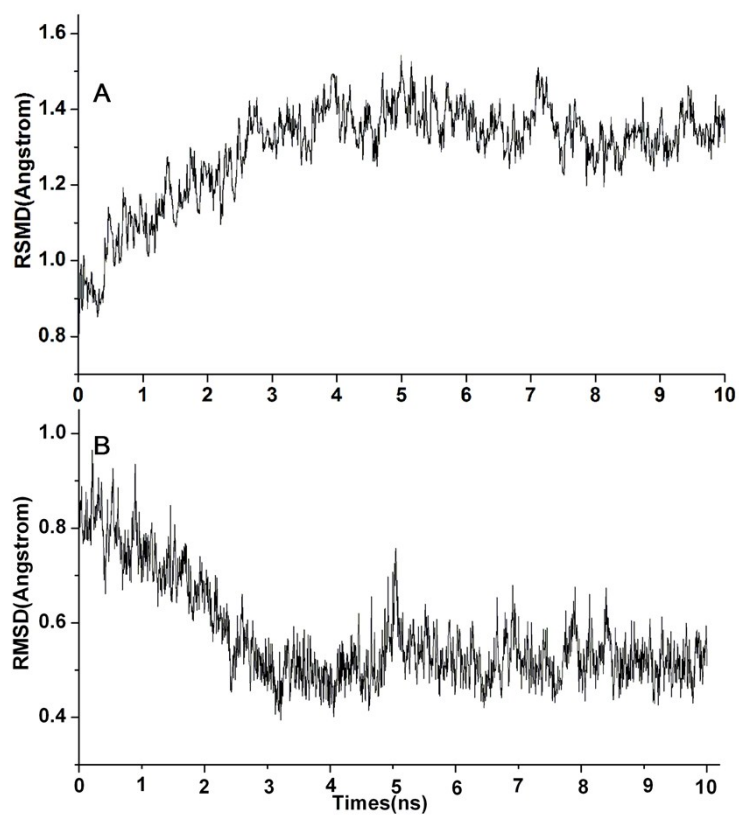


Figure S3 Time dependence of RMSD for the backbone atoms for LinD in complex with linalool (A) and β -myrcene (B) during 10 ns MD simulations.

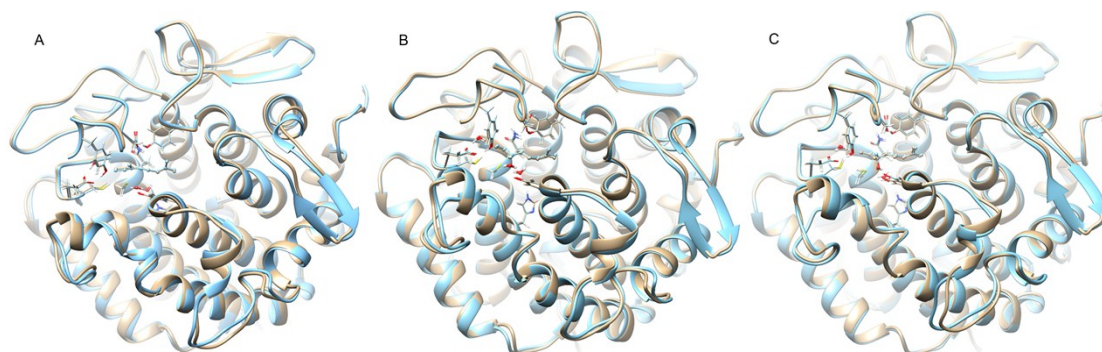


Figure S4 Superimposition of QM/MM-optimized geometries of (A) IM1 and IM1', (B) TS2 and TS2' and (C) IM2 and IM2'. The key residues in the active site are displayed in ball and stick. The structures of IM1, TS2 and IM2 are shown in brown, and the geometries of IM1', TS2' and IM2' from the QM/MM-optimized structures after molecular dynamics simulations are given in cyan. Note: IM1', TS2' and IM2' were obtained by the following procedure: First, IM1, TS2 and IM2 were energy-minimized; then, they were performed MD simulations for 2 ns with the QM regions fixed; finally, the structures extracted from the MD trajectories were conducted QM/MM optimizations. The RMSDs of IM1', TS2' and IM2' relative to IM1, TS2 and IM2 are 0.612, 0.586 and 0.603 Å, respectively.

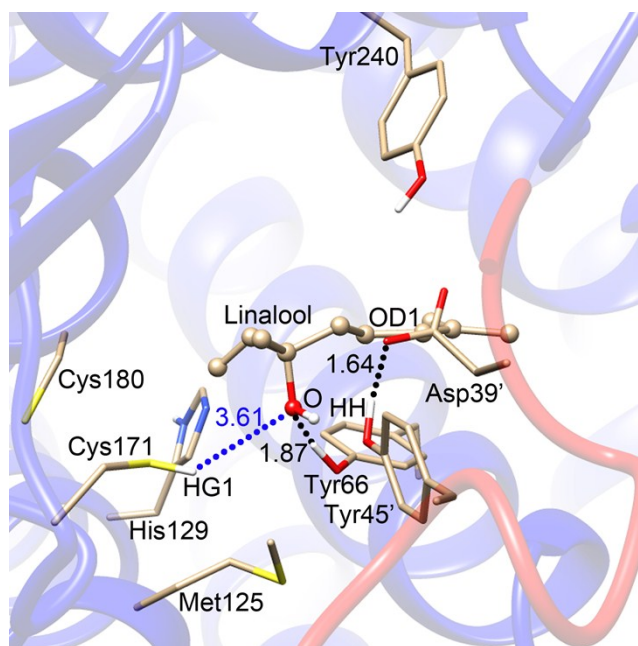


Figure S5 QM/MM-optimized geometry of the active site from LinD in complex with (*S*)-linalool. The black dashed lines represent the hydrogen bonds while the blue dashed line represents the distance between two atoms. All the distances are in angstroms.

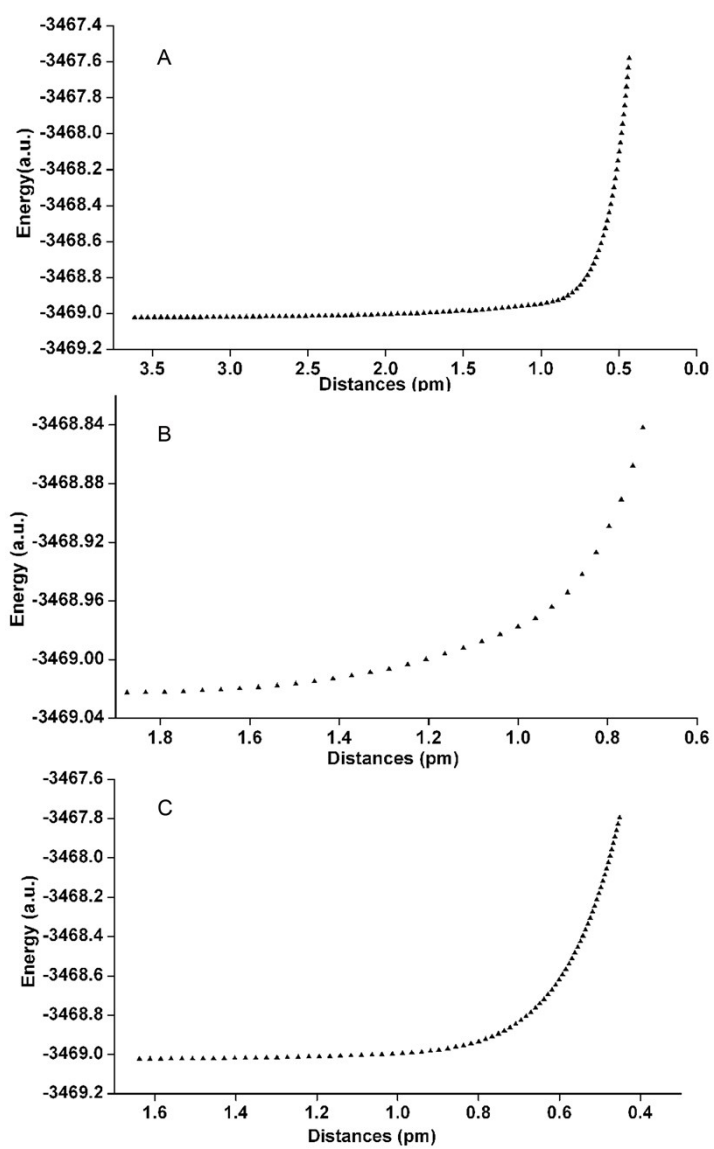


Figure S6 Scanned potential energy surfaces along the reaction coordinate in path I (A) (O of linalool and HG1 of Cys171), (B) path II (O of linalool and HH of Tyr66), and (C) path III (OG1 of Asp39' and HH of Tyr45').

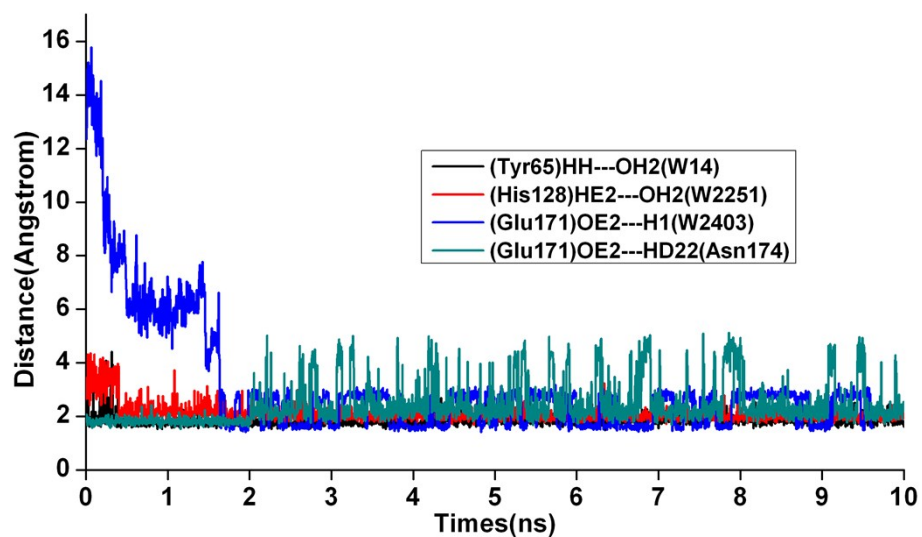


Figure S7 Time dependence of distances of three water molecules with the surrounding residues.